UNIVERSITY OF CALIFORNIA

Radiation Laboratory

Contract No. W-7405-eng-48

[redacted]

PROTON BEAM CURRENT MEASUREMENT IN THE LOW K.E.V. RANGE

Forrest Fairbrother, Jr.

(Thesis)

June 5, 1951

Berkeley, California

Abstract

Secondary charge effects from a 10 kilovolt proton beam and their effect upon beam current measurement are investigated. A collector is designed for beam current metering of a 60 kilovolt proton beam by means of charge measurement and energy measurement.

Introduction

The idea out of which this thesis grew was to measure a proton beam current, heretofore regarded as fairly large in magnitude, with an approximate energy of 60 kilovolts. The problem was then one of engineering a current measuring device for a pulsed beam of protons approximately one ampere in magnitude. Other requirements were that the device make a rapid and fairly accurate determination of the beam current.

In order to study this problem two ion sources were available. The first was a machine which gave 10 to 15 kilovolt protons in a fairly well defined beam, and current collection could be done at ground potential. The second machine accelerated protons to 60 kilovolts, and the current collection had to be done at the aforementioned potential.

The scope of this thesis is primarily to present the design and characteristics of the desired current measuring device, and secondarily to present any information about the physics of current collectors found in the process of proving the design.

Contents

Page

Abstract 3

Introduction 4

List of Illustrations 6

Chapter I Historical Background 8

Chapter II Theory of Measurement 11

Energy Measurement

Chapter III Study of Secondary Particles in a Collector 20

Design of Collector

Experimental Results

Conclusions

Chapter IV Design of a Collector to Measure a 60 Kilovolt Proton Beam 30

Requirements

Design

General Discussion of Equipment

An Estimate of Error in Measurement

Calorimetric Determination of Current

Electrical Determination of Current

Results

Conclusions and Recommendations

Bibliography 48

Appendix 49

Acknowledgments 52

List of Illustrations

Figure		Page
1	Faraday cylinder method of beam measurement	10
2a	Faraday cylinder with suppressor grid	13
2b	Collector current versus electrode potential graph	13
3a	Arrangement for calculating potential due to beam positive charge	16
3b	Normalized potential versus normalized distance from collector	16
4	Cross section of collector for studying secondary particles	21
5a	Photograph of collector for studying secondary particles	22
5b	Reverse of view in 5a	22
6	Arrangement for study of secondary charge liberated by 10 KV collector	23
7a	Collector current vs. electrode potential	26
7b		26
7c		27
7d		27
7e		28
7f		28
7g	Secondary ratios vs. collector-source distance	29
8	60 KV collector	31
9	Electrical diagram for 60 KV metering	32
10	Side of thermo-probe in high voltage liner	33
11	Exploded view of prove showing flexible cables and insulated leads	33
12	Push rods and electrical leads emerging through end vacuum seal of probe	35
13	Front view showing movable shutters and entrance grid of probe	35
14	A. C. power input to probe heater vs. galvanometer deflection	37

List of Illustrations (cont.)

Figure		Page
15	Beam current vs. collector voltage curves	42
16	Current pulse	43
17	Drop in 60 KV supply voltage during beam pulse	43
18	Electrical beam vs. thermal beam current	45
19	Normalized beam current versus cup opening	46

Chapter I

Historical Background of Measurement of Beam Currents

Before proceeding with the theory of beam current measurement it may well to present some of the methods used by other workers in meeting this same general problem.

Among the early workers the most common method of measuring beam current or charge was the use of the Faraday Cup. One of the earliest uses of such a cup was in the determination of the beam coming from a canal-ray source. In its most general sense a Faraday Cup consists of a volume enclosed by a good conducting material with a small entrance opening for the beam. With this geometry the probability of secondary charges escaping the innercup is very small.

Dujardin and Hoyaux mention in a survey article[1] that suppressor grids were used in front of the collecting surface even previous to the Faraday Cup in order to suppress secondary charges, but they do not cite any references.

When the effective diameter of beams became greater with greater current it became necessary to use a long cylinder open at one end in order to be sure of collecting all of the current. Tuve, Dahl and Hafstad[2] used Faraday cylinders a few centimeters in diameter and ten centimeters long for the aforementioned purpose. The solid angle through which secondary charges could escape the cylinder was, nevertheless, still appreciable.

Hailer[3] and Craiggs[4] solved the problem independently by the use of a Faraday cylinder and a grid at such potential as to repel incoming

---

1 Dufardin and Hoyaux, "Comparative Survey of Ion Guns", Nucleonics, 4, no. 7, 67-71 July (1949)
2 Tuve, Dahl and Hafstad, Phys. Rev. 48, 241 (1935)
3 Hailer, Wiss, Veroffenth, Siemens-Werken, 17, 321 (1937)
4 Craigs, Proc. Phys. Soc. 54, 245 (1942)

electrons and keep electrons from leaving the cylinder. The grid was placed immediately over the entrance to the cylinder.

Another method mentioned in the literature describes a magnetic trap for secondary electrons. Thoneman[5] employed a magnetic field parallel to a collecting copper surface to turn the low energy secondary electrons back to the collector.

Current in the foregoing discussion was finally read by use of a meter in series with the collector cup as shown in Fig. 1.

With the advent of larger beams, higher energy and pulse techniques of the past few years other methods of beam measurement have been found. If the beam can be sent through an ionization chamber the value of the beam current may be determined by knowledge of the number of ionizations per centimeter of path length for a known particle energy and pressure in the chamber. Monitoring the amount of radiation from the target presents us with another method of determination of the beam current. The foregoing two methods were not looked into in detail, because considerations of accuracy and geometry made their use impossible.

Research workers at the Oak Ridge National Laboratory[6] did get some figures for neutron yeilds caused by the interaction of a deuteron beam with deuterons on copper; however, the figures obtained when this same system was used to measure a 60 kilovolt deuteron beam at the University of California Radiation Laboratory were not in good agreement with those taken at Oak Ridge.

---

5 Thoneman, Nature 158, 61 (1946)
6 Y-495 Report, Electromagnetic Research Div., Carbon and Carbide Chemicals Co.

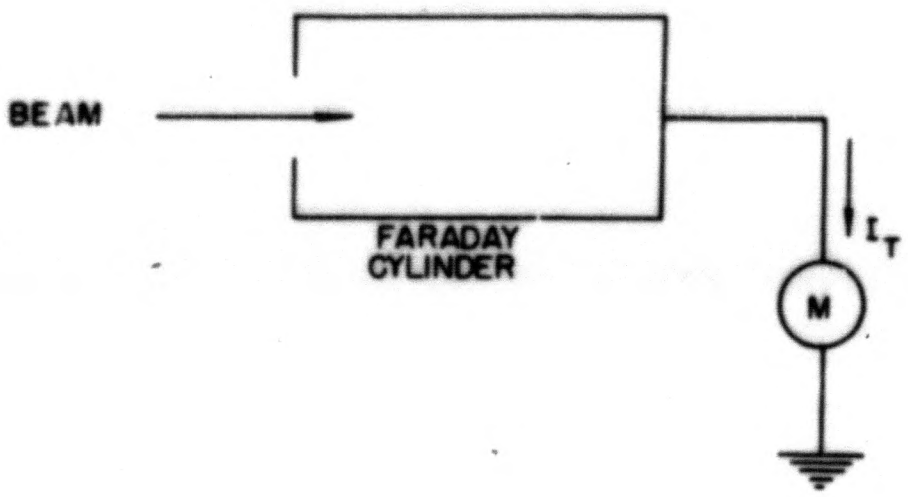

FIGURE 1. FARADAY CYLINDER METHOD
OF BEAM MEASUREMENT

MU 1984

Chapter II

Theory of Measurement

The theory of electrical measurement is quite simple. A beam of charged particles strikes a collector and finds an appropriate complete path through a current measuring device. Metered current then represents the net charge landing on and leaving the collector. For example, positive and negative charge may impinge on a surface and liberate positive and negative secondary charges. Positive current to a metering device may be constituted by positive charge landing and negative charge leaving, while negative current is just the opposite. The relationship is expressed below in formula form.

$$I_T = I_{+a} - I_{+l} - I_{-a} + I_{-l} \qquad (2\text{-}1)$$

where I_T = total positive current read on the meter

I_{+a} = current due to positive charge landing

I_{-a} = current due to negative charge landing

I_{+l} = current due to positive charge leaving

I_{-l} = current due to negative charge leaving

In getting an accurage determination of I_{+a} by reading the total current, I_T, one must either be able to reduce the other three components in equation (2-1) to a magnitude which they are negligible or be able to determine the magnitude of each of them. When I_{+a} is protons it is logical to assume that I_{+l} is very small compared to I_{+a} since the positive charges arriving effectively give up their charge to the conducting surface and become neutral atoms.(7) Our equation for the total metered current now

---

7 Dujardin and Hoyaux, "Comparative Survey of Ion Guns", Nucleonics 4, no. 7, 67-71 July (1949)

becomes:

$$I_T = I_{+a} - I_{-a} + I_{-f} \qquad (2\text{-}2)$$

The arrangement in Fig. 2a would seem to afford an ideal geometry for the determination of the unknown quantities in equation (2-2). If negative voltage were applied to the grid it would be expected that all negative secondary charge of energy less the applied voltage formed in the cup would be retained. Also negative charge directed into the cup would be turned around. If the applied potential is now made sufficiently large 99 percent or more of the negative charges will be turned around, and it may be said that $I_{-a} = I_{-ga}$, the negative charge current arriving which is formed on the grid and in the volume between the grid and cup.

$$I_{T_{-G}} = I_{+a} - I_{-ga} \qquad (2\text{-}3)$$

where $I_{T_{-G}}$ = total current read when the grid is at a negative potential with respect to ground.

When the grid is at a positive potential with respect to ground

$$I_{T_{+G}} = I_{+a} - I_{-ca} + I_{-f} \qquad (2\text{-}4)$$

where $I_{T_{+G}}$ = total current when the grid is at a positive potential with respect to ground

I_{-ca} = negative charge current collected from volume in front of the grid.

By grounding the grid and applying positive and negative potentials to the collector with regard to ground one is able to obtain expressions as below.

$$I_{T_{+c}} = I_{+a} - I_{-da} - I_{-ga} \qquad (2\text{-}5)$$

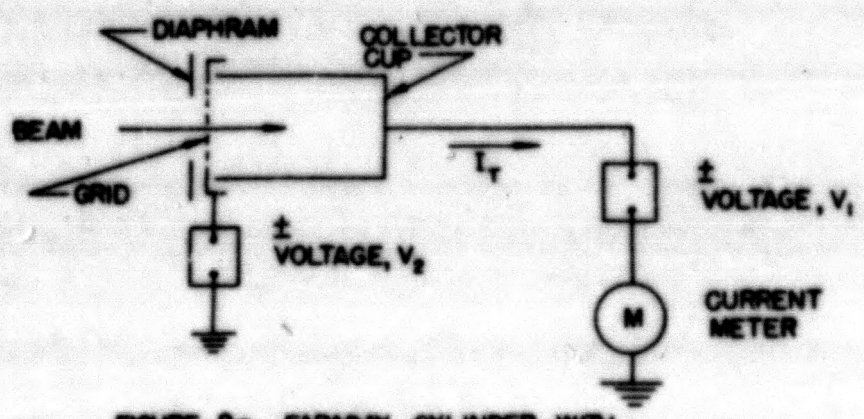

FIGURE 2a FARADAY CYLINDER WITH SUPPRESSOR GRID

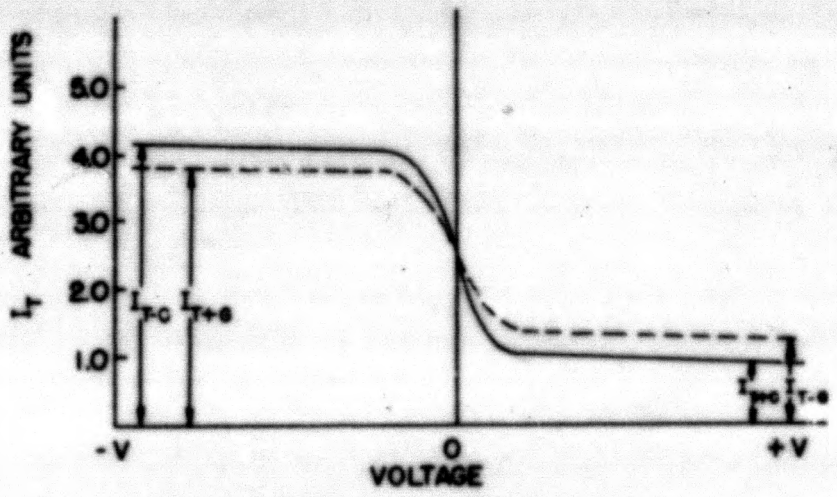

FIGURE 2b COLLECTOR CURRENT vs. ELECTRODE POTENTIAL

MU 1985

where $I_{T_{+c}}$ = total current when collector is at positive potential with respect to ground

I_{-da} = negative charge in volume in front of grid drifting onto the collector

$$I_{T_{-c}} = I_{+a} + I_{-f} \qquad (2\text{-}6)$$

$I_{T_{-c}}$ = total current when collector is at negative potential with respect to ground.

In an actual case the total current as a function of the collector voltage with respect to the grid would look as in Fig. 2b.

It can be seen by looking at equations (2-3) through (2-6) that there are four independent equations, but five unknowns. However, the endeavor can be to eliminate I_{-ga} by making the grid 98 to 99 percent transparent to the beam. Even if the secondary to primary ratio at the grid is three then the generated secondaries amount to only 3 to 6 percent of the I_{+a}. Of this amount less than half will arrive at the collector cup due to solid angle considerations.

A means is now available (at least in theory) for the determination of I_{+a}, I_{-f}, I_{-ca} and I_{-da} providing the I_{+a} versus collector voltage curves flatten in the region of large positive and negative potential, and that no other potentials exist in the region of the cup to distort the fields between the grid and cup.

One obvious source of potential is the beam of positive charges, each charge contributing a potential dV.

$$dV = \frac{dq}{\epsilon d} \qquad (2\text{-}7)$$

where dV = potential (volts)

dq = element of charge (coulombs)

ϵ = rational permittivity of space (farads/M)

d = distance from point under consideration to element of charge (meters)

therefore,

$$V = \int_0^V dV = \int_0^{d_o} \frac{dq}{\epsilon d} \tag{2-8}$$

Now consider the case of a beam of only positive charges of density ρ coulombs per cubic meter as in Fig. 3a. For ease of calculation we will consider the beam and its image charge to extend infinitely in either direction.

The problem of computing the potential on the axis due to the density ρ is much simplified if the origin of coordinates is considered to be l distant from the conducting boundary. The potential contributions from charges greater than l distant to the right or left add to be zero due to symmetry and opposite sign of the charge. Evaluation of the potential contribution from the charge density in the cylinder $2l$ in length will then give the answer as a function of l.

assuming ρ is a constant.

$$V(l) = \frac{4\pi\rho}{\epsilon}\int_0^l\int_0^{r_o} \frac{r\,dr\,dz}{\sqrt{r^2+z^2}} - \frac{2\pi\rho r_o^2}{\epsilon}\int_0^l \frac{dz}{\sqrt{r_b^2+z^2}}$$

$$V(l) = \frac{2\pi\rho r_o^2}{\epsilon}\left[\frac{l}{r_o}\sqrt{1+\left(\frac{l}{r_o}\right)^2} - \left(\frac{l}{r_o}\right)^2 + \ln\left(\frac{l}{r_o}+\sqrt{1+\left(\frac{l}{r_o}\right)^2}\right)\right.$$

$$\left. - \ln\left(\frac{l}{r_b}+\sqrt{1+\left(\frac{l}{r_o}\right)^2}\right)\right] \tag{2-9}$$

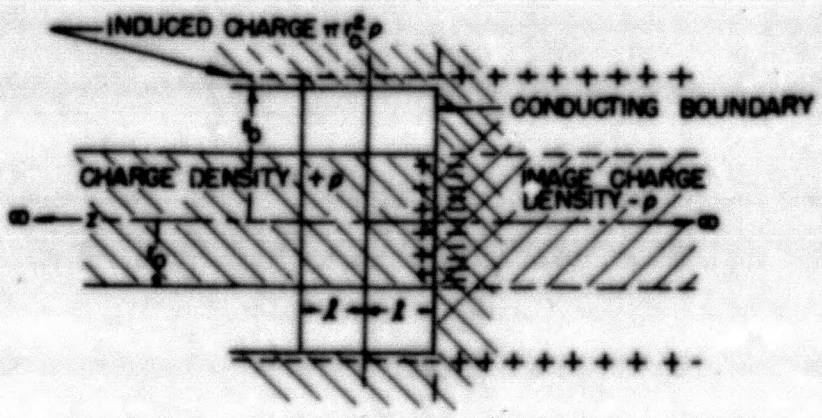

FIGURE 3a ARRANGEMENT FOR CALCULATING POTENTIAL DUE TO BEAM POSITIVE CHARGE

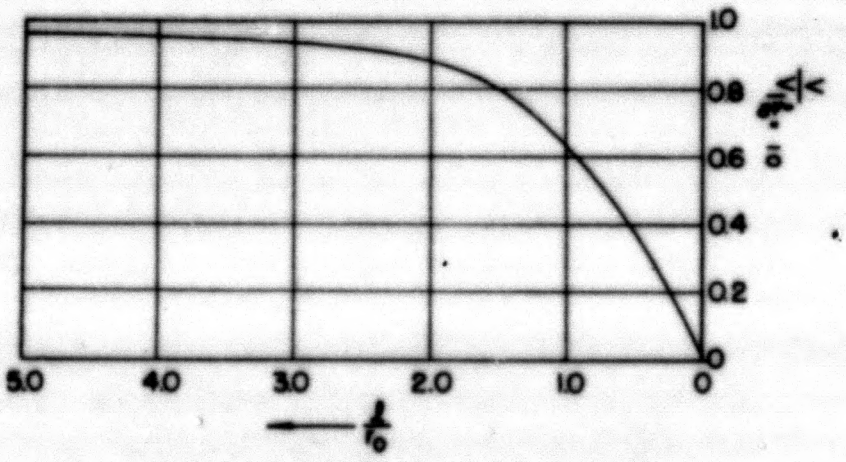

FIGURE 3b NORMALIZED POTENTIAL VERSUS NORMALIZED DISTANCE FROM COLLECTOR

MU 1986

A curve of V as a function of ℓ for $r_b = 2r_o$ is shown in Fig. 3b. For 10 kilovolt protons at a current of 100 milliamperes, $r_o = 2.5$ centimeters, the potential at $\frac{\ell}{r_o} = 10$ is 20 kilovolts or at $\frac{\ell}{r_o} = 2$ is 18 kilovolts. This might seem entirely out of line with physical experience; however, by introducing a current of negatively charged particles from the back of the cup, a portion of the charge density due to the beam of positively charged particles will be neutralized. In fact, the slower the negative particles are traveling the greater is their charge density.

$$\rho = \frac{I_s}{v} \tag{2-10}$$

where ρ = charge density due to negative particles (coulombs per cubic meter)

I_s = current per unit area (amp/M^2)

v = velocity of particles (M/sec.)

It can be qualitatively seen[8] that the negatively charged particles have the greatest charge density in the region where they are going slowest. This region will most likely be near the conducting back plate, because the potential of the beam accelerates them away from the back plate of the collector. The net result of the current and velocity of the negative particles would be to neutralize a portion of the positive charge density, and this neutralization would be strongest near the back plate. There is a high probability that the beam is partially neutralized all of the way to the source since a 20 kilovolt potential on the axes would cause a 10 kilovolt proton beam to diverge very greatly, and this phenomenon was not observed in practice.

It is also known that the energy required to accelerate n charges

---

8 Applied Electronics, MIT staff, pp.114-121, John Wiley and Sons, Inc. (1943)

into a beam is equal to their kinetic energy plus their potential energy of position at any instant.

$$E = nQV = n \times \frac{1}{2}mv^2 + \frac{1}{2}\sum_{1}^{n} C_i V_i \qquad (2\text{-}11)$$

where Q = charge on a particle (coulombs)

V = voltage through which n charges are accelerated

m = mass of one particle

v = velocity of one particle

V_i = potential at the point where i^{th} charge is located due to all other charges

E = energy to accelerate n particles into a beam

n = number of particles.

The first term of equation (2-11) represents the kinetic energy of the particles and the final term the potential energy of position.[9] Beam deflection experiments in a magnetic field have been performed in which the deflection was found to agree closely ($\pm$ 10 percent) with that predicted on the basis that V_i is negligible with respect to the accelerating voltage V.

By making ℓ/r_o small the effect of any field due to the beam charge may be minimized. Inspection of the I_T versus collector voltage curves will determine what magnitude of effect any field from the beam may have on the secondary charge.

A magnetic field perpendicular to the axis of the beam is another device by which the secondary charges may be restricted to a desired region; however, when this is done[10] it is difficult to be certain that the beam

---

9 G. P. Harnwell, Principles of Electricity and Magnetism, second edition pp. 48-49 (1949) (McGraw-Hill Book Co.)

10 Thoneman, Nature 158, 61 (1946)

potential has negligible effect upon secondary charges, since the collector current versus collector voltage will not necessarily exhibit a plateau. However, if the range of energy of the particles is known, then enough magnetic field may be applied to restrict the particles to a thin plane perpendicular to the beam axis.

Energy Measurement

Measurement of the beam current by means of the energy transmitted by the beam depends upon the evaluation of the following integral.

$$U = \int_0^t e(t)\, i(t)\, dt. \tag{2-12}$$

therefore,

$$I_{ave} = \frac{1}{t} \int_0^t i(t)\, dt = \frac{U}{\int_0^t e(t)\, dt} \tag{2-13}$$

where U = the energy delivered to the collector by the beam in time t (joules)

t = time (sec.)

$e(t)$ = the acceleration voltage as a function of time (volts)

$i(t)$ = the beam current as a function of time (amps)

I_{ave} = the average beam current over time t (amps)

Secondary electrons from the collector could subtract only approximately 0.2 percent from the total energy of a proton beam assuming all electrons received a maximum momentum from elastic collision. Due to the statistical nature of the secondary emission, the actual ratio of secondary energy to the beam energy will be something less than the above figure. Therefore, the energy determination to the desired degree of accuracy is not affected by the secondary charges.

Chapter III

Study of Secondary Particles in a Collector

Design of Collector

For the purpose of studying secondary particles due to a 10 kilovolt proton beam a collector as shown in Fig. 4 was designed. The important dimensions are the inner diameter of the collimating diaphram, 1-3/8 inches, the collector to grid spacing, 7/32 inches, and the grid to collimating diaphram spacing 1/4 inch. The grid was fashioned from a 98 percent transparent tungster grid ribbon, one inch wide. Tungsten wires one mil in diameter are spaced 0.1 inch apart in directions at right angles to each other. Photographs of the device are shown in Figs. 5a and 5b. For the experimentation described here there is no grid in the collimating diaphram, as is shown in the foregoing photographs.

By making the collector relatively shallow, ($\ell/r = 0.16$) it was hoped that the effect of the beam positive charge on secondary electrons would be negligible. It is possible that the secondary electron charge more than cancels the field due to the positive charge of the beam; (see equation (2-10)) however, since the magnitude of the foregoing effect was not known, the effort in the initial design was to cope with the effect of positive beam charge.

The surfaces of the collector were cleaned by an acid bath and light sand blasting. Physical arrangement of the source and collector are shown in Fig. 6. The details of the ion source will not be gone into here.[11] Suffice to say that the beam of 10 kilovolt protons diverged from the 1-1/2 inch diameter exit grid assembly by an angle of approximately 16 degrees, and operated pulsed on for 2 milliseconds once every second. Current was determined by

---

11 Ion source developed by John Foster. University of California Radiation Laboratory, Berkeley, California.

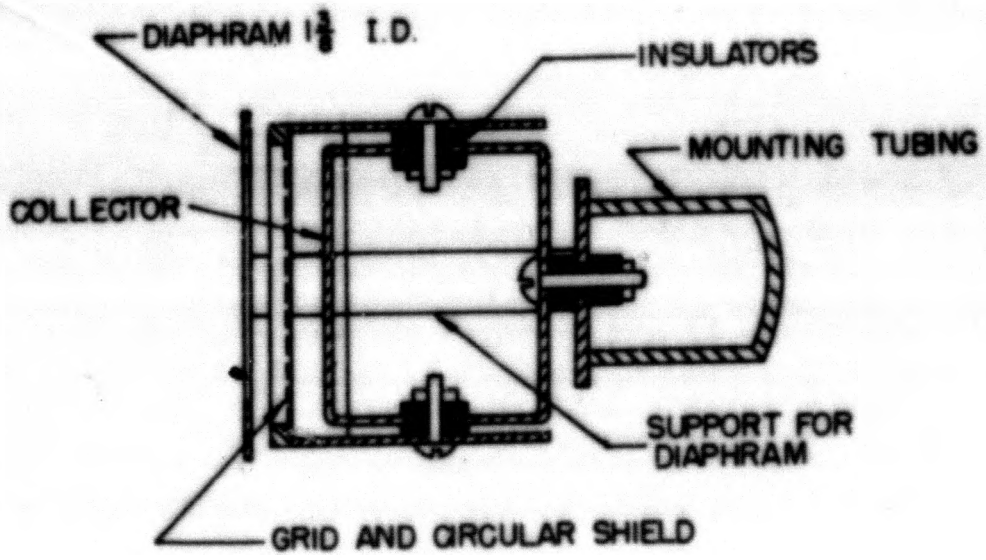

FIGURE 4 CROSS SECTION OF COLLECTOR FOR STUDYING SECONDARY PARTICLES

MU 1987

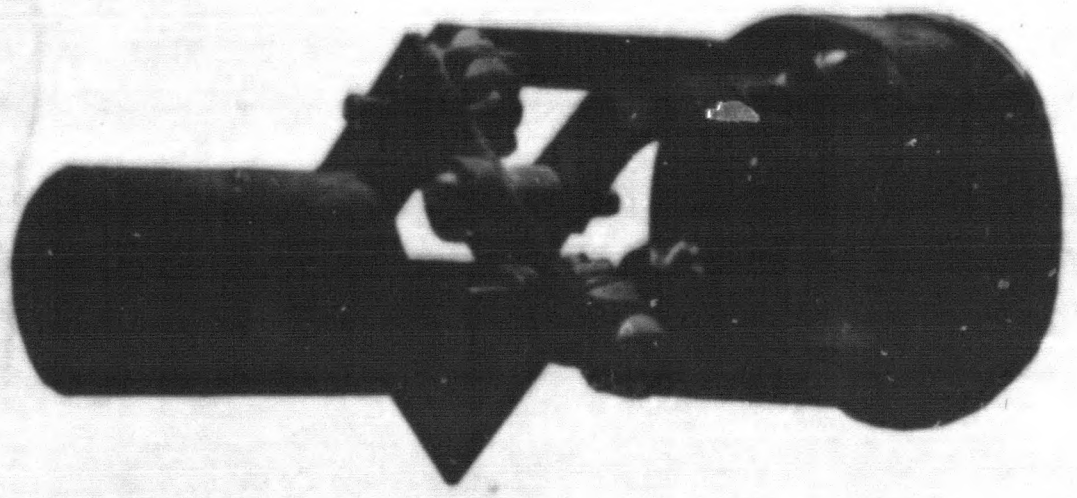

COLLECTOR FOR STUDY OF SECONDARY PARTICLES
FIGURE 5a

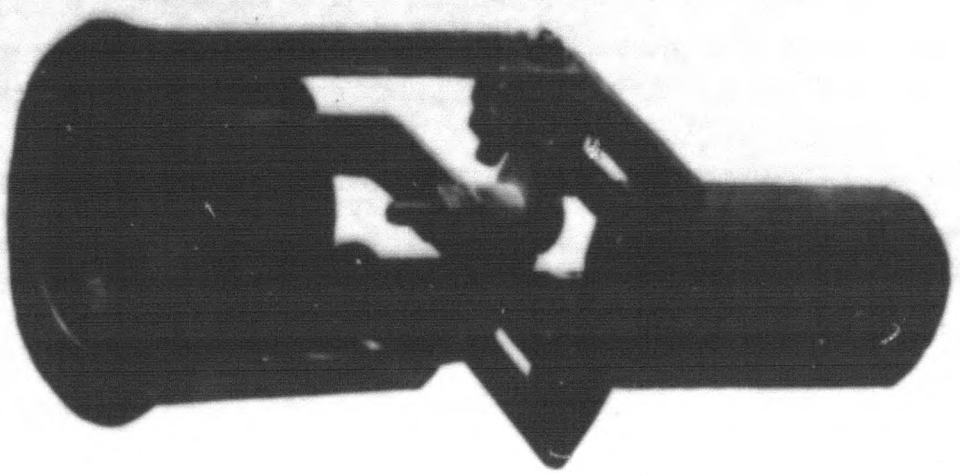

REVERSE VIEW OF 5a
FIGURE 5b

OZ 1121

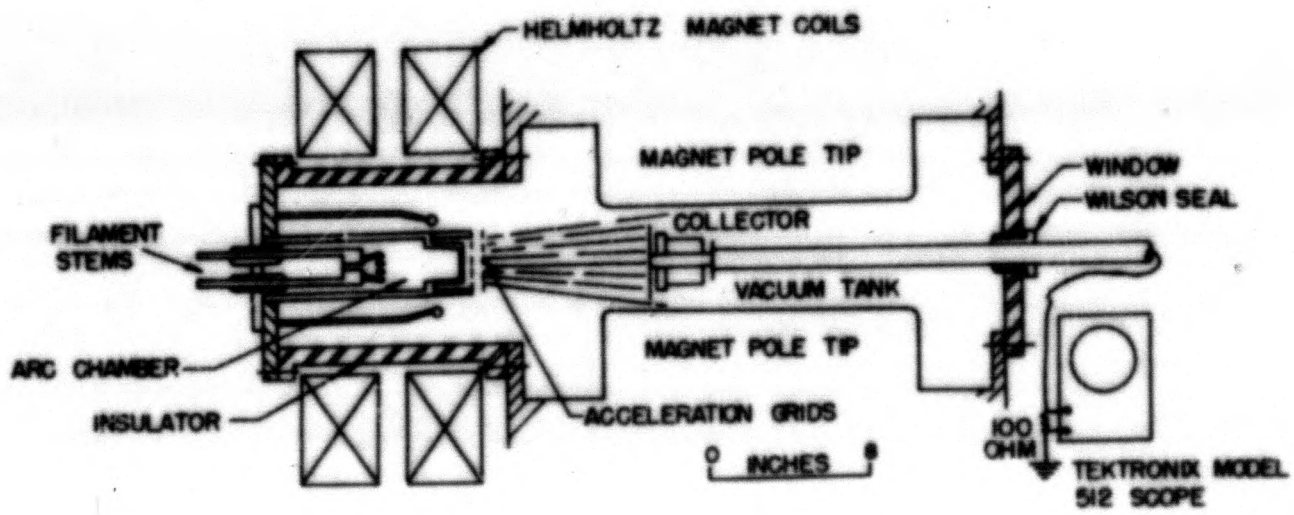

FIGURE 6 ARRANGEMENT FOR STUDY OF SECONDARY CHARGE LIBERATED BY 10 KV PROTON BEAM

MU 1989

reading on a cathode ray oscillograph the voltage pulse across a 100 ohm resistor inserted in series with the element to be metered, i.e., collector, grid, or diaphram.

Experimental Results

The solution to equations (2-3) through (2-6) are shown below.

$$I_{+a} = I_{T_{-G}} \tag{2-14}$$

$$I_{-l} = I_{T_{-c}} - I_{+a} \tag{2-15}$$

$$I_{-ca} = I_{T_{-c}} - I_{T_{+G}} \tag{2-16}$$

$$I_{-da} = I_{T_{-G}} - I_{T_{+c}} \tag{2-17}$$

Since the above solutions are possible only when $I_{-ga} = 0$, an attempt was made to justify this assumption. Data taken with and without magnetic field across the collector is presented in Fig. 7f. Figs. 7a and 7b present experimental curves, as outlined in chapter II when the cup has been operated one half hour and two and one-half hours respectively. Figs. 7c, d and e show the same curves at different collector positions. Summary of results is shown in Figs. 7f and Table I, where the ratio of the negative charge current leaving the collector to positive arriving, the negative charge current collected from volume in front of the grid to the positive arriving, and the negative charge in the volume in front of grid drifting toward the collector to the positive arriving are shown as a function of collector distance.

Conclusions

The negative charge leaving the grid and striking the collector was proved to be negligible when the curves in Fig. 7e coincided for positive collector voltages. The presence of 400 gauss magnetic field in a plane perpendicular to the beam axis effectively prevents any electrons formed at

the grid (the larmor radius for a 20 volt electron is 0.0148 inches) from reaching the collector, therefore, if there is no change in the current versus collector voltage curve (at positive voltages) when magnetic field is removed it follows that secondary charge from the grid is not appreciable.

The decrease in the ratio of negative secondary charges leaving to incident positive charges with operating time has been shown by other workers to be characteristic of vacuum systems that are not clean.(12) However, an effect that was not understood was the increase in the above ratio with increasing collector distance. It is believed that this effect is intimately tied up with the fact that the collector current could not be made to show a plateau characteristic (Fig. 7d) when the collector was 20 inches from the source. Also not understood but believed connected with the above affect is the increase of the ratio of negative charge collected in front of the grid to incident positive charge with increasing collector distances.

Since the secondary ratio is essentially constant at 4.5 and 8 inches collector distance, it is felt that the true ratio was determined at the foregoing distances, and is 1.75 ± 0.15.

The author found no data in the literature for a comparison with the above figure; however, a secondary ratio of 3.84 for a 18 kilovolt proton beam impinging upon copper surface that was not specially cleaned was recorded by Hill, Bruechner, Clark and Fisk.(12)

---

12 Hill, A. G., Bruechner, W. W., Clark, J. S and Fisk, J. B., Phys. Rev. 55, 463 (1939)

COLLECTOR CURRENT vs. ELECTRODE POTENTIAL

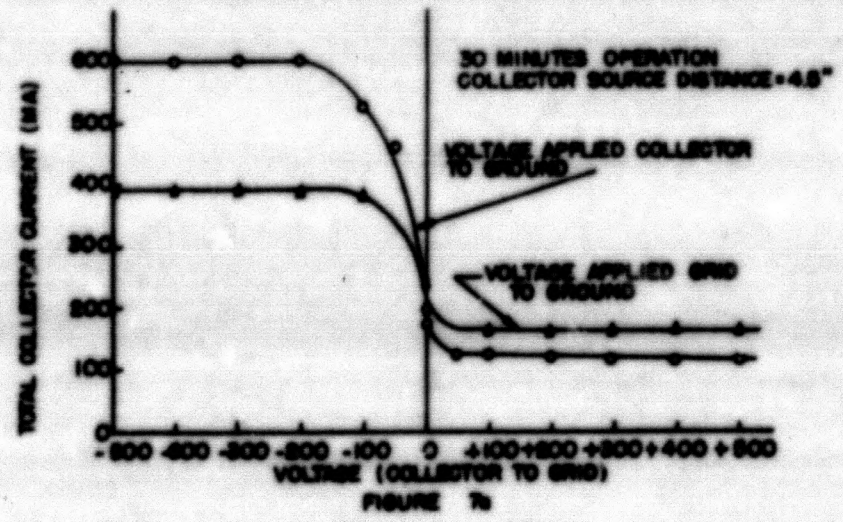

FIGURE 7a

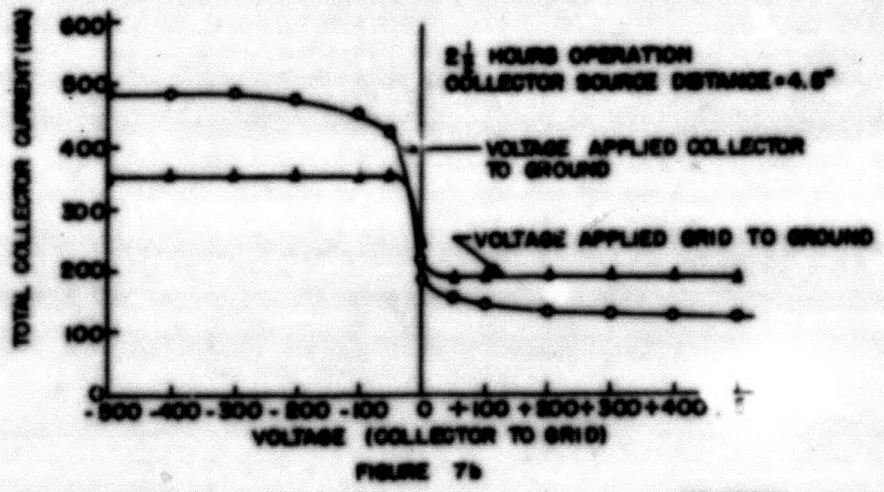

FIGURE 7b

MU 1989

COLLECTOR CURRENT vs ELECTRODE POTENTIAL

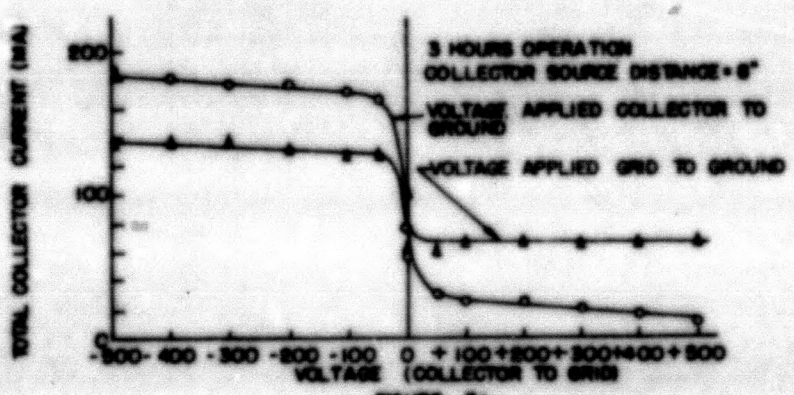

FIGURE 7c

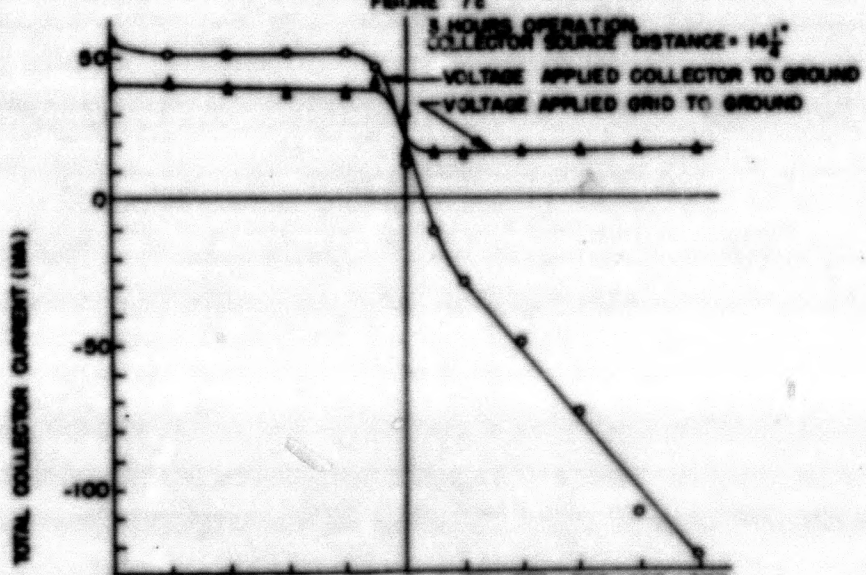

FIGURE 7d

MJ 1990

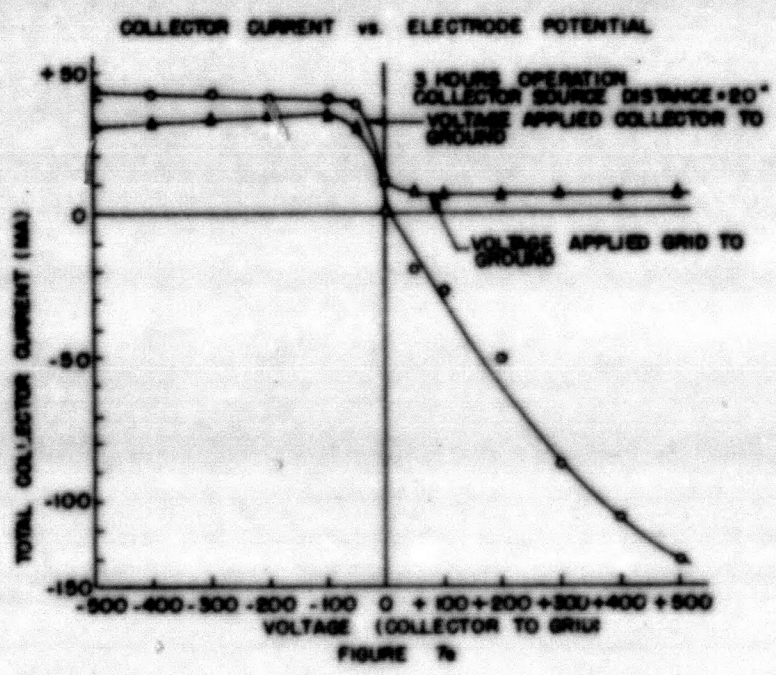

FIGURE 7e

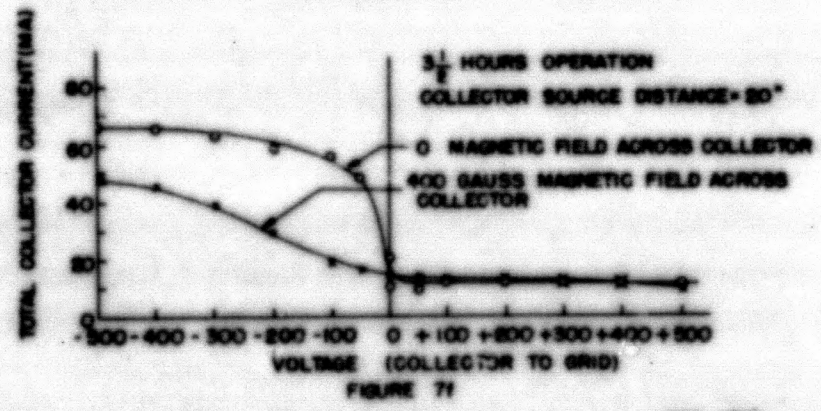

FIGURE 7f

MU 1991

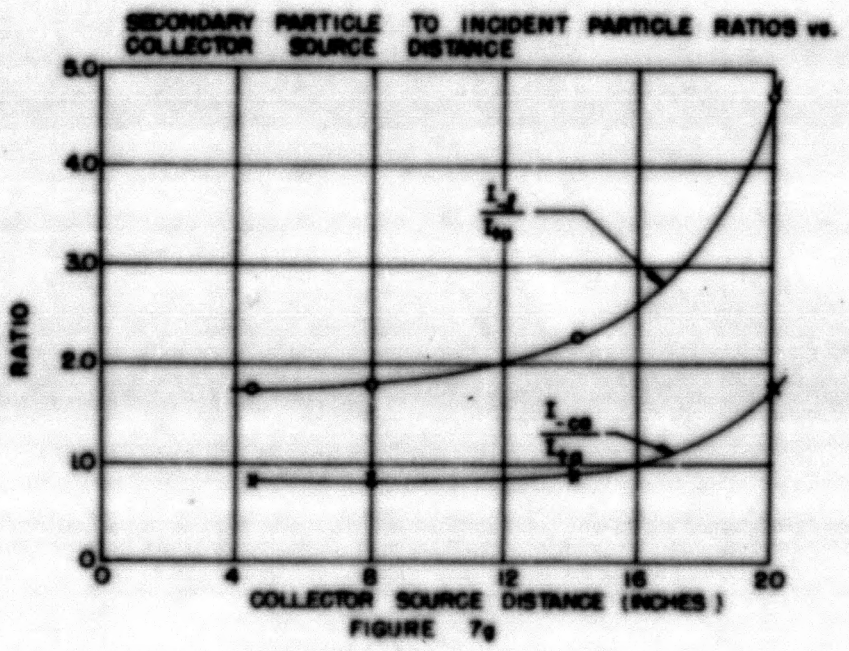

FIGURE 7g

TABLE I

	4	2½	3	3	3
	4.5	4.5	0	14½	20
$\frac{I_{-2}}{I_{+0}}$	2.75	1.7	1.8	2.2	4.7
$\frac{I_{-.05}}{I_{+0}}$	1.5	0.76	0.77	0.88	1.75
$\frac{I_{-.05}}{I_{+0}}$	0.31	0.35	0.85	—	—

MU 1992

Chapter IV

Desi[illegible] of a Collector to Measure a 60 Kilovolt Proton Beam

Requirements

The requirements were that the collector be able to make measurements rapidly and fairly accurately of a pulsed proton beam current of approximately one ampere peak. It was also desired to be able to control the aperture of the collector from without the vacuum tank in order to study the beam density, and to be able to move the collector along the axis of the beam without breaking vacuum.

Design

It was decided that the requirement of rapid measurement was best satisfied by measuring the charge landing on a shielded collector in the presence of magnetic field perpendicular to the beam axis. This was supplemented by a calorimetric determination of the beam energy which was used for the purpose of calibrating the charge measurement.

Fig. 8 shows overall design of the collector cup. The inner cup was three inches deep and backed by a four by four inch piece of copper which accomodated a heating element. Copper tubing conducted heat away from the collector to a copper block which was water cooled by vacuum tight coaxial tubing. The beam hitting the back of the collector caused a temperature rise which was read by a copper-constantin thermocouple and galvanometer connected across the conducting section. When the beam was turned off a.c. power was applied to the heater until the temperature rise across the conducting section was the same as observed with the beam striking the collector. The conducting section was two inches long, one inch in diameter with a wall thickness of 0.0625 inches, and gave approximately 100° C temperature rise for eighty watts average power. Current was determined directly by inserting a ten ohm resistor

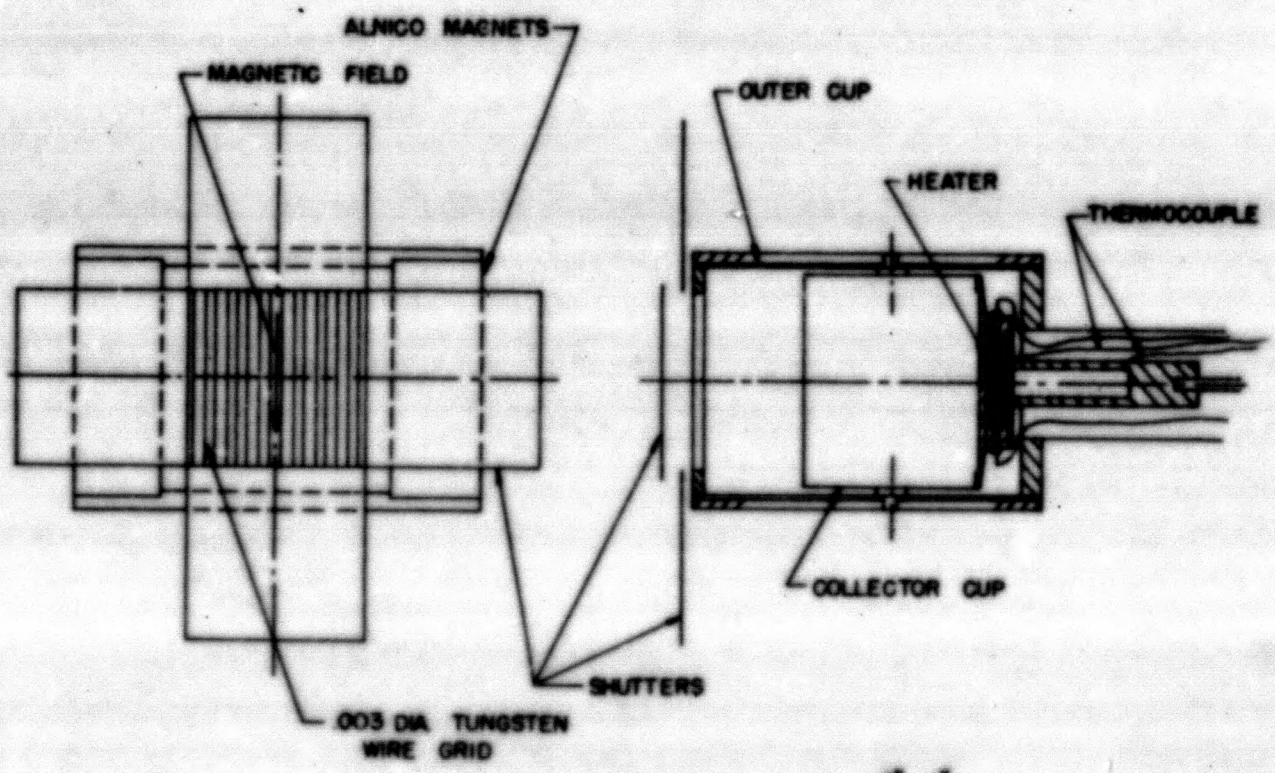

FIGURE 8 60 KV COLLECTOR

MU 1993

ELECTRICAL DIAGRAM FOR ENERGY AND CURRENT DETERMINATION

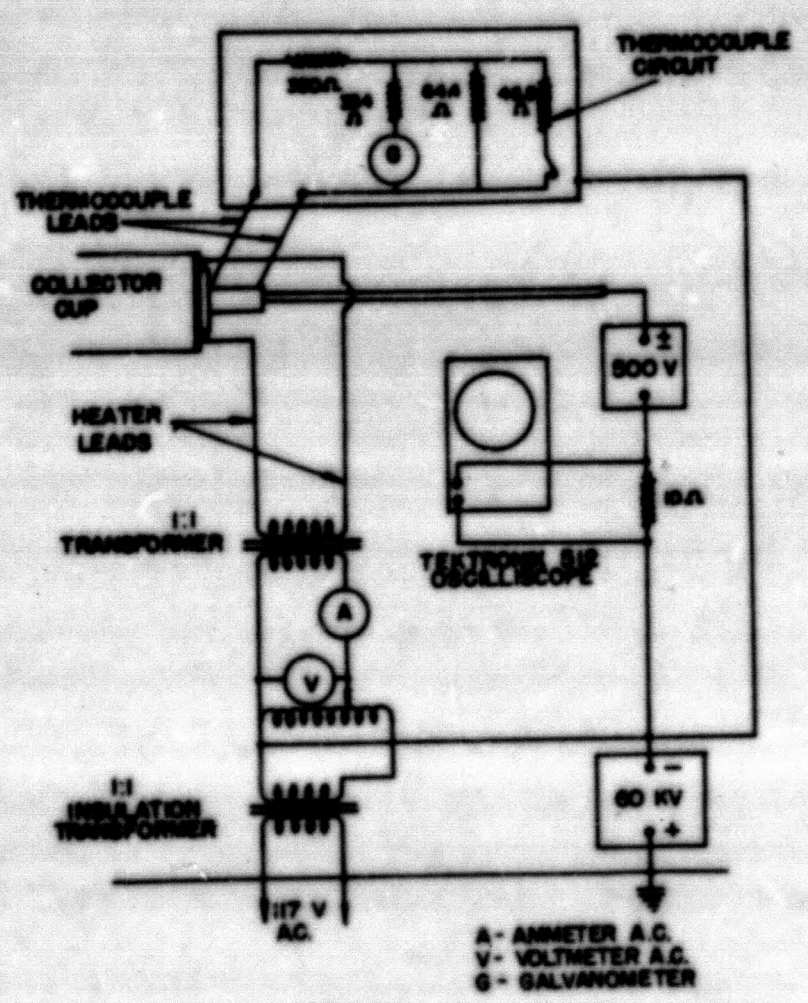

FIGURE 9 ELECTRICAL DIAGRAM FOR 60 KV METERING

MU 1994

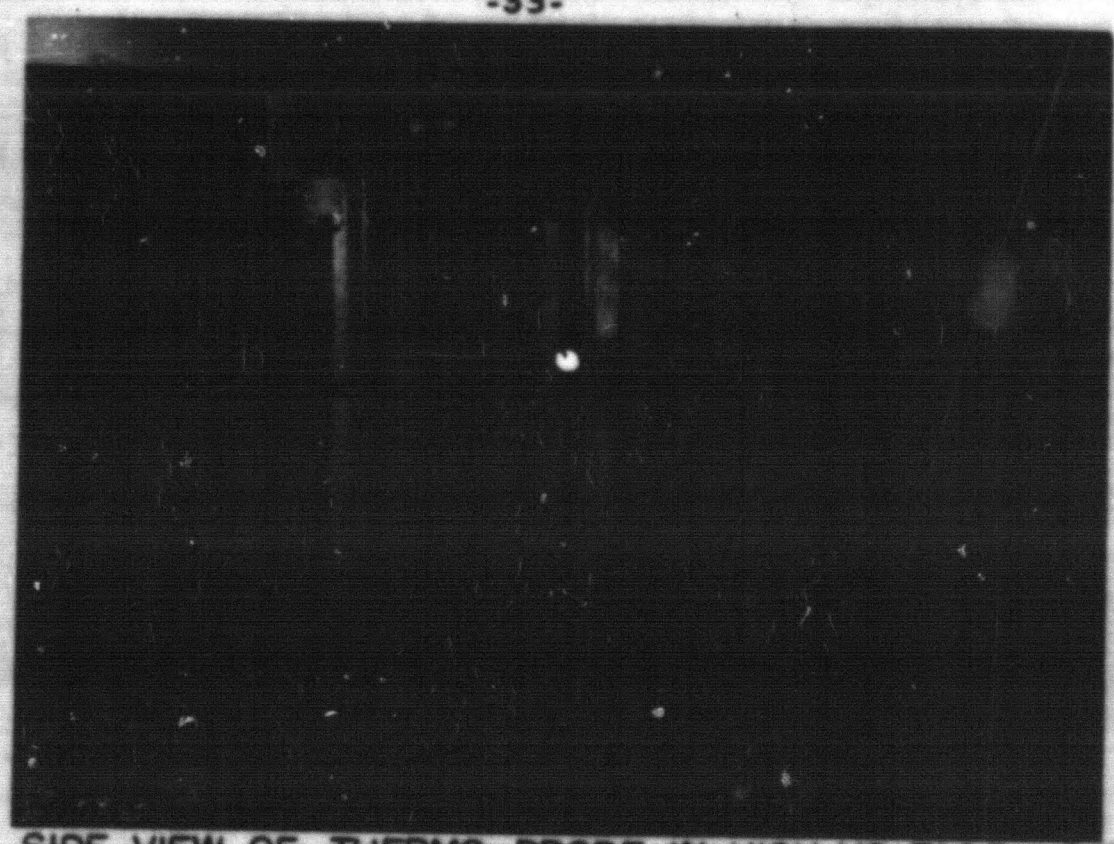

SIDE VIEW OF THERMO-PROBE IN HIGH VOLTAGE LINER
FIGURE 10

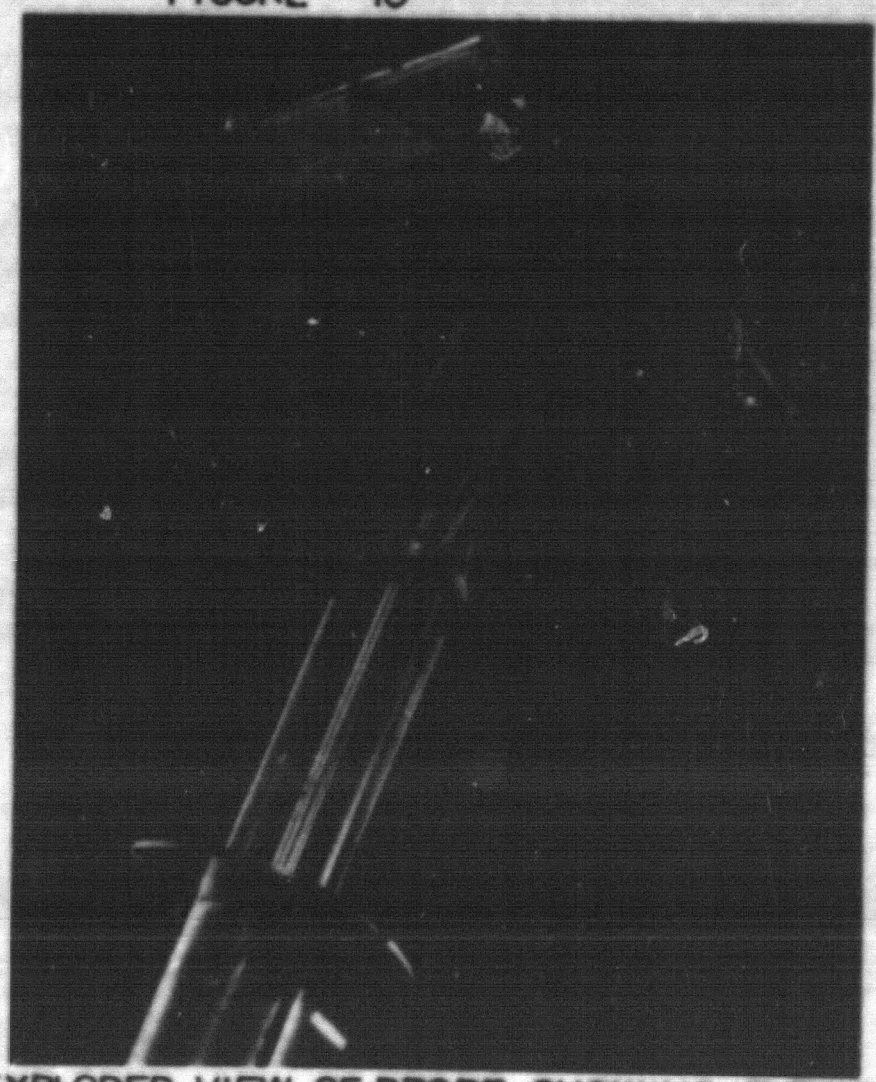

EXPLODED VIEW OF PROBE SHOWING FLEXIBLE AND INSULATED LEADS
FIGURE 11

OZ 1122

in series with the collector cup and reading the resultant voltage pulse with an oscilloscope. Details of the electrical system are shown in Fig. 9. It should be noted that all metering had to be done at -60 kilovolts, necessitating isolating transformers and platforms on standoff insulators for the placing of meters and scopes. All high voltage equipment was placed in a screened area, and meters, etc., had to be read from approximately 18 inches distance.

Potential was applied to the collector with respect to the shield for the purpose of aiding the magnetic field in holding secondary charges in the cup. Since the anticipated charge density of the beam entering the cup was so high (greater than one amp in a four inch diameter) compared with the value used in the ten kilovolt measurement of chapter II, it was decided to use sufficient magnetic field to restrict secondard charge to a thin disc volume perpendicular to the beam. The magnetic field across the collector was supplied by four two by two by six inch alnico permanent magnets mounted around the cup by an iron yoke (see Fig. 10). The field strength at the center of the cup was 290 gauss, and at the shutters was 242 gauss.

A space of one and three-quarters inches was maintained between the shutters and the entrance to the cup in order that secondary charges formed at the grid should not strike the collector. The radius for 100 volt electrons in a 250 gauss magnetic field is only 0.053 inches, and the penetration in crossed magnetic and electric fields caused by 500 volts on the collector is approximately 0.005 inches; however, the electric field in the region of the grid need have only a small component parallel to the magnetic field for some of the negative charges formed at the grid to arrive at the collector. The foregoing dimensions were necessary to minimize such a possibility. Spacings are shown in Fig. 8.

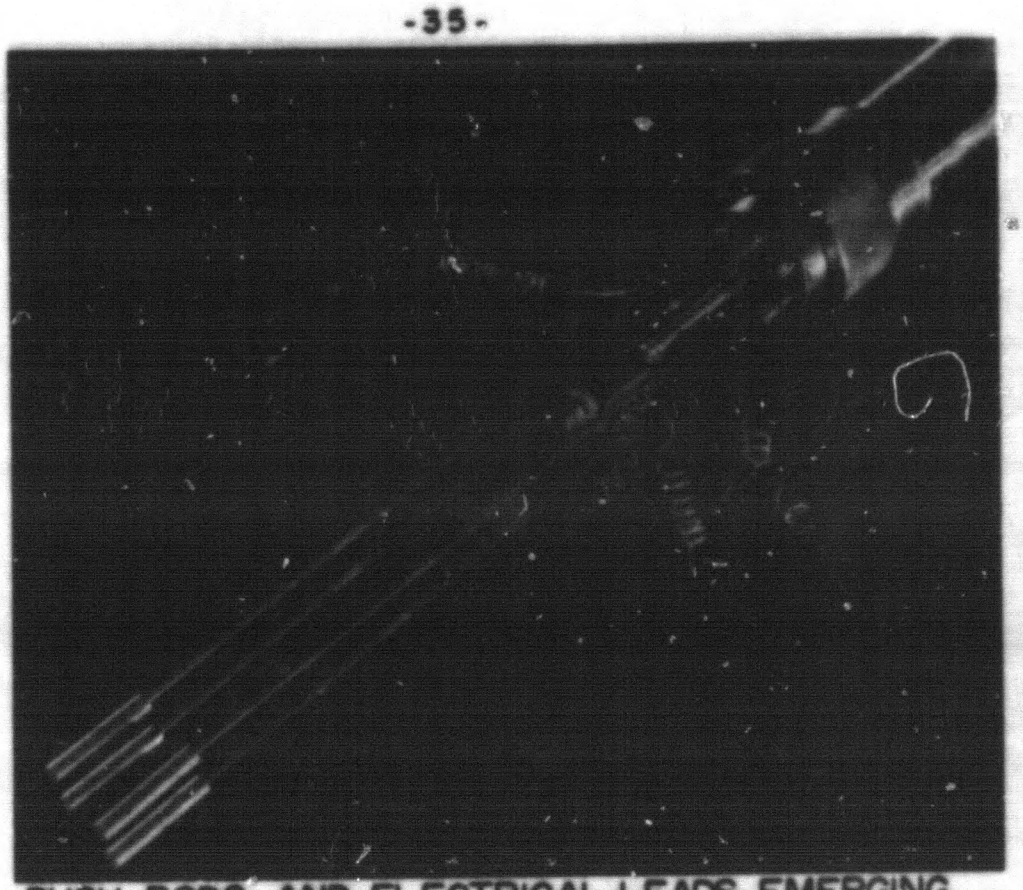

PUSH RODS AND ELECTRICAL LEADS EMERGING THROUGH END VACUUM SEAL OF PROBE
FIGURE 12

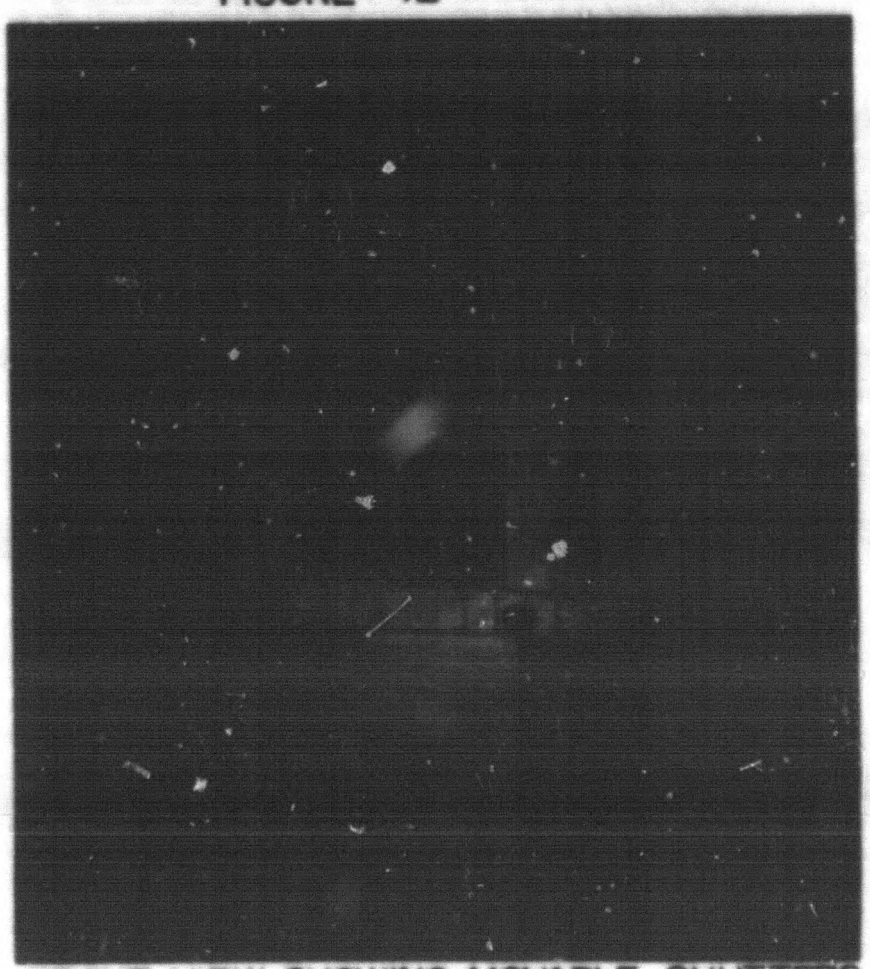

FRONT VIEW SHOWING MOVABLE SHUTTERS AND ENTRANCE GRID OF PROBE.
FIGURE 13

The shutters are four by four by one-sixteenth inch stainless steel plates, sliding in brass channels, and actuated by means of piano wires in flexible cables. One-eight inch diameter stainless steel rods connect to the piano wire and transfer the motion from outside the vacuum tank through "O" ring seals. The connection of the flexible cables to the guide tubing for the one-eight inch rods is shown in Fig. 11, and the rods emerging from the "O" ring seals in Fig. 12. Figure 13 illustrates the front of the cup with shutters opened.

Feedthrough kovar seals pass the wiring and water tubes through bulkheads in the two inch outer diameter stainless steel guide tubing (see Fig. 12). The vacuum seal for wiring and water tubes of the two inch tubing is also accomplished by use of kovar seals. Sealing the two inch tube to the sub assembly of pushrods, wiring and watertubing was done by using a rubber "O" ring and threaded compression ring (see Fig. 13).

The collector with magnets attached weighed approximately fifty pounds, and therefore had to be supported by wheels and rails. An overhead rail system of two "U" channels facing each other provided surface for wheels attached to the top of the magnet yoke. A second point of support (though the weight supported was small) was the chevron seal through which the two inch tubing moved in and out.

General Discussion of Equipment

For the purpose of calibration the thermal determination was used. Energy spread of the particles had been found by magnetic deflection to be small enough to be negligible compared to the accuracy of the current determination. The beam contained some molecular ions, and these were not discriminated in the measurement since both protons and molecular ions received

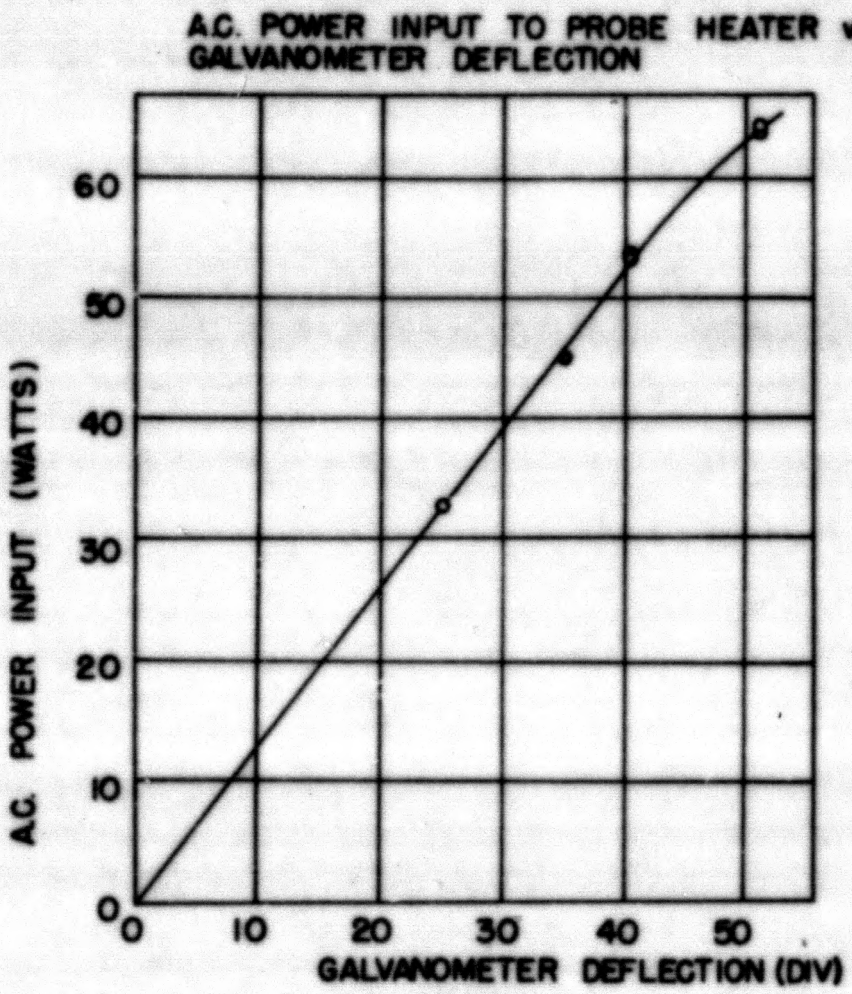

FIGURE 14

MU 1995

the same energy.

A graph was made of the galvanometer deflection versus the a.c. power input to the heating element (see Fig. 14). This facilitated thermal determinations of the beam current, since one needed only to wait for the beam to bring the galvanometer to equilibrium and read the power input from the aforementioned graph. The pulse repetition rate was determined by scaling the power frequency (60 cycles per second) down with an electronic binary scaler. Pulse length was determined by calibrating the scope sweep with a 1000 cycle tuning fork stable to plus or minus 0.05 percent. Calibration of the tuning fork itself was accomplished by comparison with the power frequency, and done to plus or minus 0.1 percent.

Tektronix model 512 oscilloscopes were used, and the voltage calibration was checked to plus or minus 1.0 percent by means of a laboratory voltmeter. The accelerating voltage was determined by reading the voltage on a panel meter to which the supply charged, and then subtracting the voltage drop, read on a scope, due to the incident beam current. This procedure was necessary since the d.c. reading of the scope seemed to drift due to corona on the compensated divider. Total maximum error in calibration was $\pm$ 1.9 percent. A. c. curent and voltage applied to the heating element were read on precision a.c. laboratory type meters calibrated to a maximum error of $\pm$ 1.0 percent.

Thermal equilibrium was obtained in approximately one half hour when the beam repetition rate was one pulse per second.

An Estimate of Error in Measurement

Calorimetric Determination of Current.

The analysis was made on the basis of a maximum possible error (calibration etc.) and a probable error in reading instruments. The reason for this hybrid basis of error is the fact that meters are calibrated for a maximum possible error and hence are non-gaussian in nature. Current was determined as in equation (2-13), reprinted below.

$$I_{ave} = \frac{1}{t}\int_0^t i(t)dt = \frac{U}{\int_0^t e(t)dt} \qquad (2\text{-}13)$$

where U = energy delivered to the collector by the beam in time t (joules)

t = time of pulse (sec.)

e(t) = acceleration voltage as a function of time (volts)

i(t) = beam current as a function of time (amps)

I_{ave} = the average beam current over the time t (amps)

now, $U = E\,I\,T$ (3-1)

where E = a.c. voltage applied to the heater element

I = a.c. current in heating element (amps)

T = period of the pulse repitition rate (sec.)

therefore,

$$I_{ave} = \frac{E\,I\,T}{\int_0^t e(t)dt} \qquad (3\text{-}2)$$

Below in Table II are listed the maximum possible errors in the quantities defined in equation (3-2).

TABLE II

Quantity	Max. Pos. Error (%)
E	± 1.0
I	± 1.0
T	± 0.1
e(t)	± 1.9
t	± 0.05
I_{ave}	± 4.05

Table III below lists the probable errors in reading the equipment associated with the quantities in equation (3-2).

TABLE III

Quantity	Probable error in reading (%)
E	± 0.5
I	± 0.5
T	---
e(t)	± 1.0
t	± 2.0
I_{ave}	± 2.35

Electrical Determination of Current.

For the electrical determination it was only necessary to read a voltage pulse on a scope and divide this voltage by the resistance across which the voltage was read.

Maximum possible error in calibration of scope and associated circuits . . . . . ± 2.0%

Probable error in reading scope . . . . . ± 5.0%

Results

After the cup was bombarded steadily by the beam for a period of approximately one hour the current readings came to equilibrium. A series of collector current versus collector voltage curves for various beam values are shown in Fig. 15. It should be noted that the curves do not have the characteristic flattening for values of voltage greater than $\pm$ 200 volts. This is due to the magnetic field preventing the collector and beam potential from respectively repelling and attracting all secondary electrons.

A careful comparison of the calorimetric beam determination and the charge beam determination was made by photographing the respective pulse shapes on the oscilliscope. In this manner $\int_0^t e(t)dt$ and $\frac{1}{t}\int_0^t i(t)dt$ (equation (2-13)) were determined. The photographs are shown in Figs. 16 and 17. Table IV shows the values obtained by the use of the photographic technique.

TABLE IV

Thermal Determination

t	0.936 milliseconds
$\int_0^t e(t)dt$	0.936 x 47.5 second kilovolts
EI	58.5 watts
T	2.133 seconds
I_{ave}	2.81 $\pm$ 0.18 amperes

Charge Determination

I_{ave}	3.0 $\pm$ 0.21 amperes

From the above values of the average current it may be said that the two methods agree within the error of the measurement.

When calorimetric determination was made without the aid of photographs the average accelerating voltage and beam current were estimated

TYPICAL BEAM CURRENT vs. COLLECTOR VOLTAGE CURVES

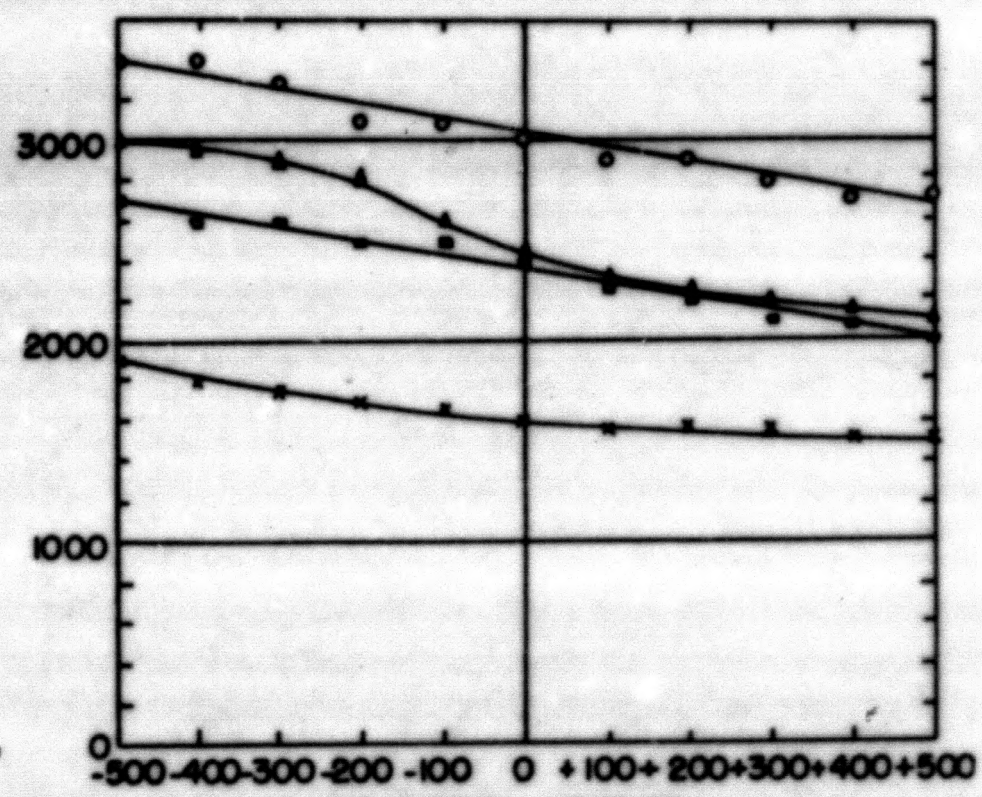

FIGURE 15

MU 1996

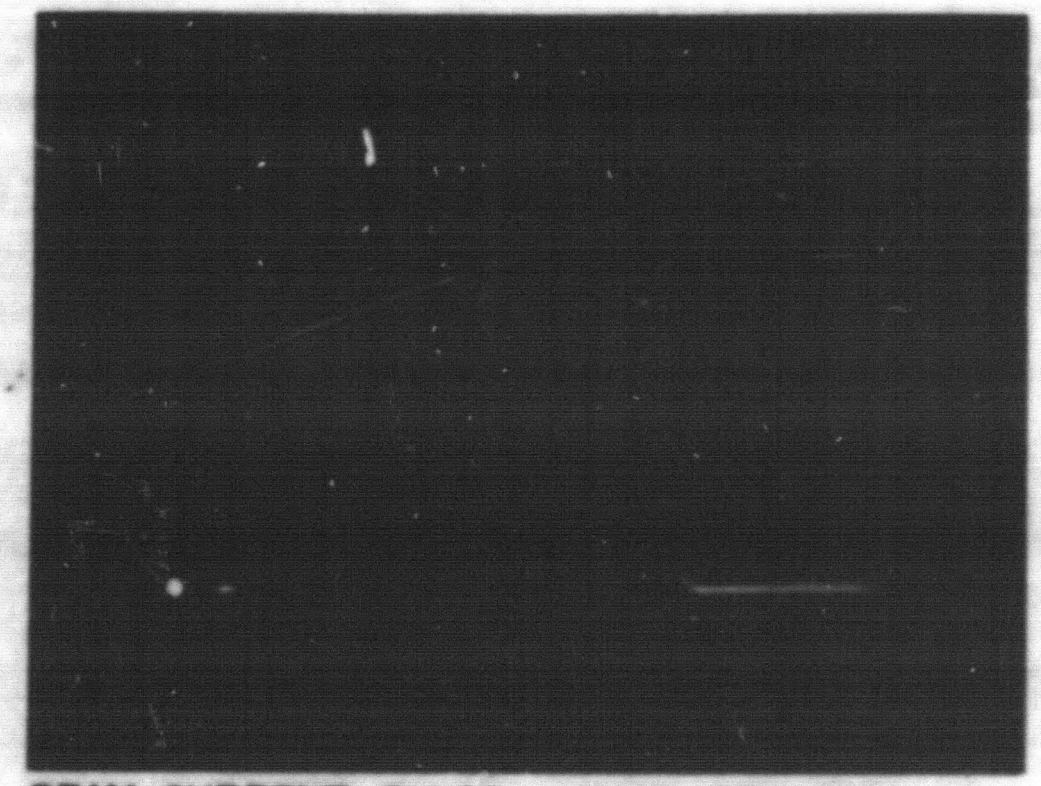

BEAM CURRENT PULSE. 1 AMP PER DIV.
FIGURE 16

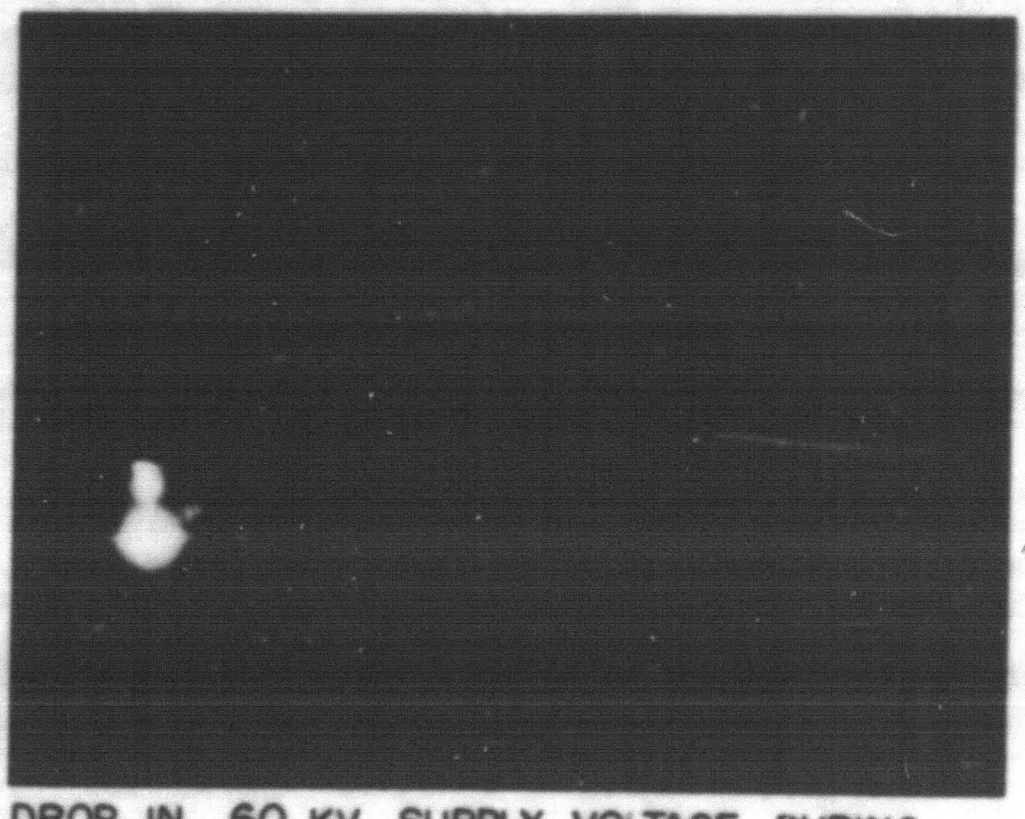

DROP IN 60 KV SUPPLY VOLTAGE DURING BEAM PULSE
FIGURE 17

visually. This resulted in an error in the calorimetric method of approximately ± 10 percent. A curve of the beam by charge determination versus beam by thermal determination is shown in Fig. 18. This curve was obtained by letting five people make approximately an equal number of determinations. All deviations are within the ± 10 percent of the thermal method and ± 7 percent of the electrical method.

As the cup opening is increased by opening the shutters a curve of beam current versus cup area is obtained as in Fig. 19.

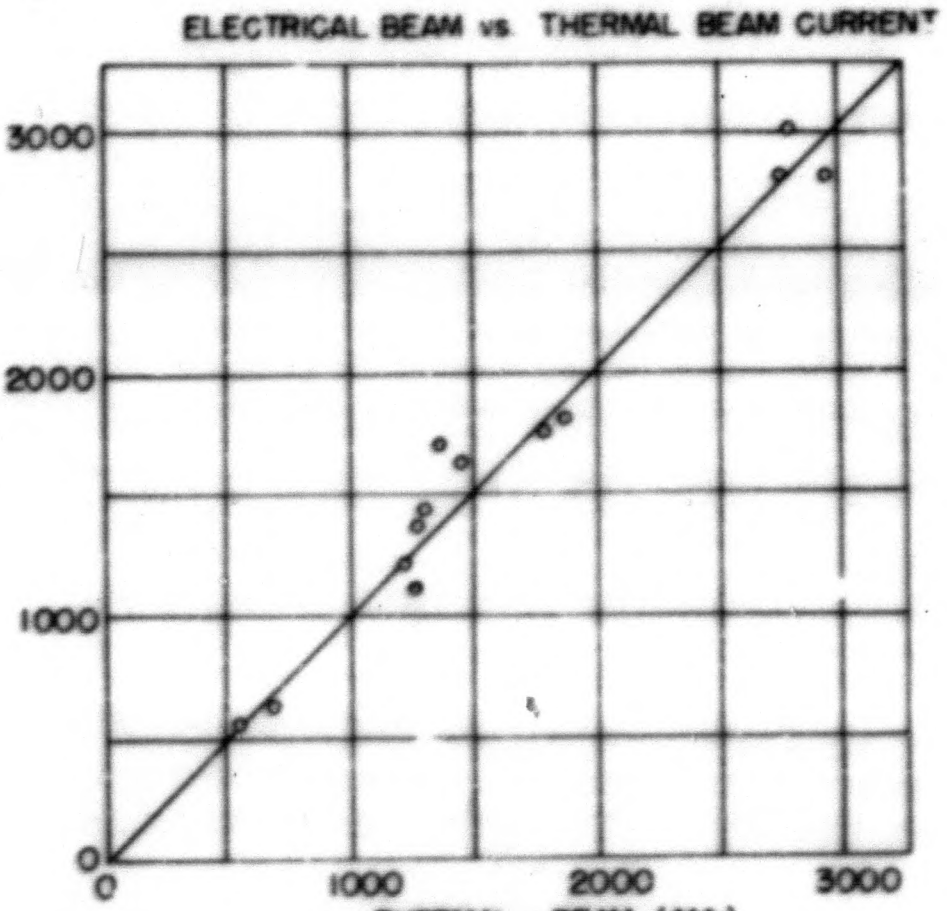

FIGURE 18

MU 1997

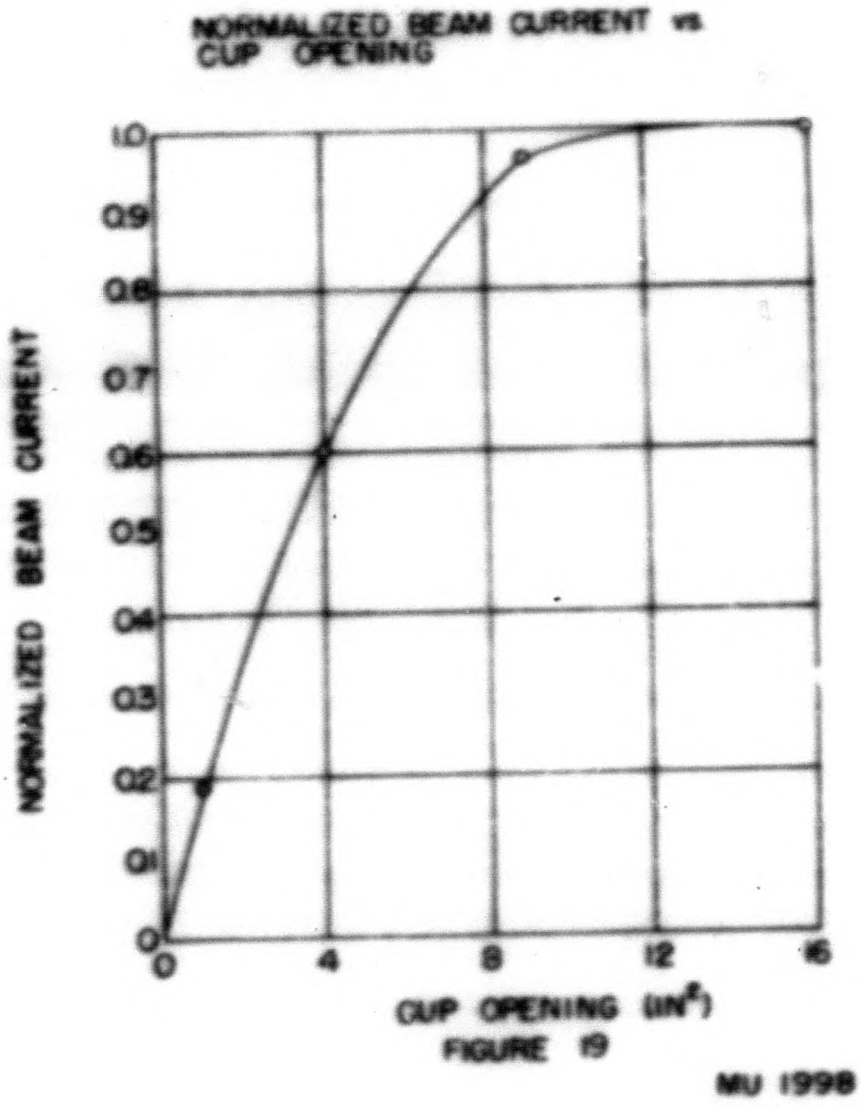

FIGURE 19

MU 1998

Conclusions and Recommendations

From the foregoing results it can be said that the value of the beam determined electrically (+ 500 volts on the collector) is the same as the value of the beam determined thermally. When the thermal determination is made by averaging pulses visually (Fig. 18) the error is less than 10 percent. The charge determination has an error of ± 7 percent of the thermal determination value; therefore, the total error of electrical determination is less than 17 percent for rapid determinations and less than 13 percent for careful determination with the aid of photographs.

The beam versus cup area geometry does not have the advantage of cylindrical symmetry, though it does have odd-even symmetry. The flattening tendency of the curve in Fig. 19 does show that most of the beam is entering a four by four inch square opening. The interpretation of this geometry is therefore mostly valuable for finding the total beam entering a given square area in preference to the beam density obtained from cylindrical geometry.

It is recommended that a system such as in Chapter II (electrostatic biasing of collector grids) is not used when duty cycles are large enough to cause the beam to heat the grids to incandescence, since the grids will then emit electrons. Systems as in Chapter III with magnetic fields to trap the electrons at the emitting grid would seem far superior, because the electrons are then trapped in a plane perpendicular to the beam axis and of thickness determined by the Larmor radius. A magnetic trap collector may be made with reasonable assurance before installation that will measure true beam current, but an electrostatic collector has a factor of uncertainty regarding its ability to measure true beam current.

Bibliography

1. Craigs, Proc. Phys. Soc. 54, 245 (1942)
2. Fowler and Gibson, Phys. Rev. 46, 1075 (1934)
3. Hailer, Wiss. Veroffenth, Siemens-Werken 17, 321 (1937)
4. Hill, A. G., Bruechner, W.W., Clark, J. S. and Fisk, J. B., Phys. Rev. 55, 463 (1939)
5. Hoyaux, Max and Dujardin, Ignace, Nucleonics 4, Nos. 5, 6, and 7 (1949)
6. Thoneman, Nature 158, 61 (19[illegible])
7. Tuve, Dahl and Hafstad, Phys. Rev. 48, 241 (1935)
8. Y-495 Report, Electromagnetic Research Division of Carbon and Carbide Chemical Corporation.
9. Applied Electronics, M.I.T. Staff, pp. 114-121, John Wiley and Son Inc. (1943)
10. Harnwell, G. P., Principles of Electricity and Magnetism, second edition, 48-49 (1949) McGraw-Hill Book Co.

An extended bibliography on current collection and ion sources in general may be found at the end of reference 5 above.

Appendix

1. Calculation of radius of curvature of electron in magnetic field.

$$\rho = \frac{1}{B}\sqrt{2\frac{m_e}{Q_e}V}$$

ρ = radius of curvature of electron (M)

B = magnetic field (webers/M^2)

m_e = mass of electron (Kg)

Q_e = charge on electron (coulombs)

V = voltage through which electron has been accelerated prior to entering magnetic field

for B = 400 gauss = 0.04 (webers/M^2)

V = 20 volts

$$\rho = \frac{1}{0.04}\sqrt{\frac{2\ (20)}{1.76 \times 10^{11}}} = 3.75 \times 10^{-4} M = 0.375 \text{ mm} = 0.0148 \text{ in.}$$

for B = 250 gauss = 0.025 (webers/M^2)

V = 100 volts

$$\rho = \frac{1}{0.025}\sqrt{\frac{2\ (100)}{1.76 \times 10^{11}}} = 1.34 \times 10^{-3} M = 1.34 \text{ mm} = 0.053 \text{ in.}$$

2. Calculation of distance penetration by electron into crossed electric and magnetic field.

$$y = \frac{2E}{B^2 \frac{Q_e}{m_e} d}$$

y = maximum penetration (M)

E = voltage between parallel plane electrodes

d = distance between parallel plane electrodes (M)

for E = 500 volts

d = 2.5 inches = 2.5 x 0.0254 = 0.0632 meters

B = 250 gauss = 0.025 (webers/M^2)

$$y = \frac{2\,(500)}{(2.5)^2 \times 10^{-4} \quad 1.76 \times 10^{11} \quad 6.32 \times 10^{-2}}$$

$= 0.1435 \times 10^{-3}$ M = 0.1435 mm = 0.00562 in.

3. Calculations for design of thermo-electric probe.

a. Determination of heat lost from radiation when probe is 100° C above room temperature.

$Q = AK (T_1^4 - T_o^4)$

A = radiating area of probe (cm^2) 4 x 4 x $(2.54)^2$ x 2 = 207 cm^2

ϵ = emmisivity of copper, assumed = 1.0.

K = Steffan Boltzman Constant = 5.7×10^{-12} (watts/cm^2 $^oC^4$)

T_o = 293° K

T_1 393° K

$Q = (393^4 - 293^4)\ 5.7 \times 10^{-12} \times 207 = 19.0$ watts.

Q_1 = total average power to probe from beam = 80 watts.

$\frac{Q}{Q_1} = \frac{19.0}{80.0} = 0.238$

therefore, 23.8 percent of total power is radiated from probe, for $\epsilon = 1.0$

b. Determination of length of conduction section.

$$\ell = \frac{AK_1\ \Delta T}{Q}$$

ℓ = length of section cm

A = area of cross section cm^2

K_1 = conductivity of copper = 3.84 $\frac{\text{watts}}{\text{cm } ^oC}$

$\Delta T = T_1 - T_o$ (^oC)

for 1 inch O.D. tubing by 0.0625 wall thickness

$$A = \frac{11}{16} \times \pi \times 1 = 0.196 \text{ in.}^2 = 1.27 \text{ cm}^2$$

$$\Delta T = 393 - 293 = 100^\circ \text{ C}$$

$$Q = 80 \text{ watts}$$

$$l = \frac{1.27 \times 3.84 \times 100}{80} = 6.1 \text{ cm} = 2.4 \text{ in.}$$

Acknowledgements

The author wishes to thank the thesis committee, Dr. J. R. Woodyard, Dr. L. W. Alvarez, and Dr. D. H. Sloan, for their interest. To Dr. E. J. Lofgren and John Foster I am indebted for many valuable suggestions during the early phases of the experimentation.

This work was performed under the auspices of the Atomic Energy Commission.

END